G Model
JMST-1139; No. of Pages 11

ARTICLE IN PRESS

Journal of Materials Science & Technology xxx (2017) xxx–xxx

Contents lists available at ScienceDirect

Journal of Materials Science & Technology

journal homepage: www.jmst.org

Microstructures and mechanical properties of friction stir welds on 9% Cr reduced activation ferritic/martensitic steel

Chao Zhang [a,b], Lei Cui [a,b,*], Yongchang Liu [a,b,*], Chenxi Liu [a,b], Huijun Li [a,b]

[a] State Key Lab of Hydraulic Engineering Simulation and Safety, School of Materials Science & Engineering, Tianjin University, Tianjin, 300354, China
[b] Tianjin Key Laboratory of Advanced Joining Technology, School of Materials Science and Engineering, Tianjin University, Tianjin, 300354, China

ARTICLE INFO

Article history:
Received 4 April 2017
Received in revised form 4 August 2017
Accepted 28 August 2017
Available online xxx

Keywords:
Friction stir welding
Reduced activation ferritic/martensitic steel
Microstructure evolution
Impact toughness

ABSTRACT

In this study, the microstructures and mechanical properties of 9%Cr reduced activation ferritic/martensitic (RAFM) steel friction stir welded joints were investigated. When a W-Re tool is used, the recommended welding parameters are 300 rpm rotational speed, 60 mm/min welding speed and 10 kn axial force. In stir zone (SZ), austenite dynamic recrystallization induced by plastic deformation and the high cooling rates lead to an obvious refinement of prior austenite grains and martensite laths. The microstructure in SZ contains lath martensite with high dislocation density, a lot of nano-sized *MX* and M_3C phase particles, but almost no $M_{23}C_6$ precipitates. In thermal mechanically affect zone (TMAZ) and heat affect zone (HAZ), refinement of prior austenite and martensitic laths and partial dissolution of $M_{23}C_6$ precipitates are obtained at relatively low rotational speed. However, with the increase of heat input, coarsening of martensitic laths, prior austenite grains, and complete dissolution of $M_{23}C_6$ precipitates are achieved. Impact toughness of SZ at −20 °C is slightly lower than that of base material (BM), and exhibits a decreasing trend with the increase of rotational speed.

1. Introduction

Reduced activation ferritic/martensitic (RAFM) steels with high chromium content (about 9 wt%) were developed to achieve high creep resistance at elevated temperatures for fossil fuel and nuclear power industries [1,2]. The microstructures of high Cr RAFM steels are generally of tempered martensite with dispersed $M_{23}C_6$ and *MX* compounds and high density of dislocations [3,4]. It can be strengthened by many approaches including precipitation hardening, solid solution hardening, dislocation hardening, and boundary or sub-boundary hardening [1]. When welding RAFM steels, the welding thermal process always introduces a degradation of the microstructure and property in the weld regions, leading to an acceleration of the joint creep damage in high temperature and stress service conditions [5,6].

Friction stir welding (FSW), a solid-state welding process, was being increasingly attractive for fabricating some weld structures to meet high temperature service conditions in nuclear power industries [7,8]. The FSW process produces a very low heat input and without any melting of materials in weld [9], and therefore some disadvantages in conventional fusion welding such as porosities, inclusions, grain and precipitates coarsening might be avoided [10,11]. Moreover, the recent improvement in FSW tool materials, such as W–Re alloy and polycrystalline cubic boron nitride (PCBN), have enlarge the field of applications for welding steels [12–14].

Previous works reported that the FSW weldability of reduced activation ferritic/martensitic steels is good and revealed the potentiality for achieving high quality welds [8,15–17]. The microstructures and properties of FSW joints on RAFM steels may show much difference compared with that of fusion welding technologies due to the special FSW process, which is based on frictional heating, plastic flow and plastic deformation of the materials in weld regions [16,18,19]. However, some key details for FSW of RAFM steels on the respects of microstructure and mechanical property are still unclear. In this study, RAFM steel plates in 5 mm thick were used for FSW experiments. By optimizing the FSW parameters, several defect-free joints were obtained. And then, the grain structure, precipitate evolution and some mechanical properties of the weld regions were systematically investigated.

* Corresponding authors at: State Key Lab of Hydraulic Engineering Simulation and Safety, School of Materials Science & Engineering, Tianjin University, Tianjin, 300354, China

E-mail addresses: leicui@tju.edu.cn (L. Cui), licmtju@vip.163.com (Y. Liu).

https://doi.org/10.1016/j.jmst.2017.11.049
1005-0302/

Please cite this article in press as: C. Zhang, et al., J. Mater. Sci. Technol. (2017), https://doi.org/10.1016/j.jmst.2017.11.049

Table 1
Chemical composition of the experimental steel (wt%).

C	Cr	Mn	V	W	Ta	Si	Zr	N	S	P	Fe
0.1	9	0.5	0.2	1.5	0.15	0.05	0.005	0.007	<0.002	<0.002	Bal.

2. Experimental procedures

Several RAFM steel plates in thickness of 5 mm were used as the base material (BM) for FSW experiment. The chemical composition of BM is shown in Table 1. Before welding, the hot rolled plates were normalized at 1000 °C for 60 min, and then water quenched for obtaining lath martensite microstructure. They were then tempered at 700 °C for 60 min for making tempered microstructures containing $M_{23}C_6$ particles dispersed at grain boundaries and *MX* particles within grains. The original microstructure of the BM is shown in Fig. 1.

The FSW experiment was conducted on an FSW-3LM-020 welding equipment produced by China Friction Stir Welding Center. The welding tool was made of W–25%Re alloy, which has a threaded taper probe in 4.7 mm length and a concave spiral shoulder in a diameter of 18 mm. The welding parameters are 200, 300 and 400 rpm tool rotational speeds, 60 mm/min welding speed, 2.5° tool tilt angle, and 10 kn axial load.

To distinguish the microstructures and inspect weld defects of the obtained joints, the as-welded specimens were cross-sectioned, ground, and mechanically polished. After being etched with a solution of 5 g $FeCl_3$, 20 mL HCl and 100 mL water, macro metallographic and microstructure observations were carried out with an OLYMPUS GX51 optical microscope. For a further observation, TDCLSU 1510 tungsten filament scanning electron microscope (SEM) was used to examine the grain structures and the $M_{23}C_6$ particle distribution features. Transmission electron microscopy (TEM) was then performed using a Tecnai G2F30 microscope to explore the characteristics of substructures and precipitates evolutions of the welds in detail. Charpy V-notch impact testing for stir zone of the weld was conducted at −20 °C on sub-sized (3.3 mm × 10 mm × 55 mm) specimens with the dimensions as shown in Fig. 2.

3. Results

3.1. Weld appearance

The cross sections of the joints obtained in all the welding parameters are shown in Fig. 3. The whole FSW weld of RAFM steel is divided into four regions as marked in Fig. 3(a)–(c): base material (BM), stir zone (SZ), thermal mechanically affected zone (TMAZ), and heat affect zone (HAZ). The SZ of the joint refers to the region where tool probe traversed and its surroundings of where the material was highly plastically deformed and recrystallized. The TMAZ refers to the region near SZ and under the tool shoulder where hot plastic deformation and material flow can also be performed during the welding process. Between TMAZ and BM, there is a region of HAZ, which experiences a welding thermal cycle and some kinds of microstructure variations, but without any plastic deformations.

The cross-sectioning observations show that the joints welded with 300 rpm and 400 rpm rotational speeds are defect-free. When rotational speed decreases to 200 rpm, tunnel type defects would form near the bottom in SZ at retreating side (RS). To all the obtained welds, the HAZs in advancing side (AS) are all wider than in RS. It is also found that, the weld appearance would show significant differences in the extent of material flow and widths of HAZ at AS with the variation of welding parameters. As shown in Fig. 3(a)–(c), the area of SZ and flow band near AS in SZ are enlarging with the increase of rotational speed. It indicates that the material flow during FSW becomes more sufficient when the tool rotational speed is increased. To the size of HAZ, an obvious variation is found at AS of the welds. The variation trend observed in the study is that the width of HAZ at AS is increased from 1.06 to 2.12 mm with the increase of rotational speed from 200 to 400 rpm,

Based on the above results, it is concluded that FSW process for RAMF steel can be performed successfully with a W–Re tool

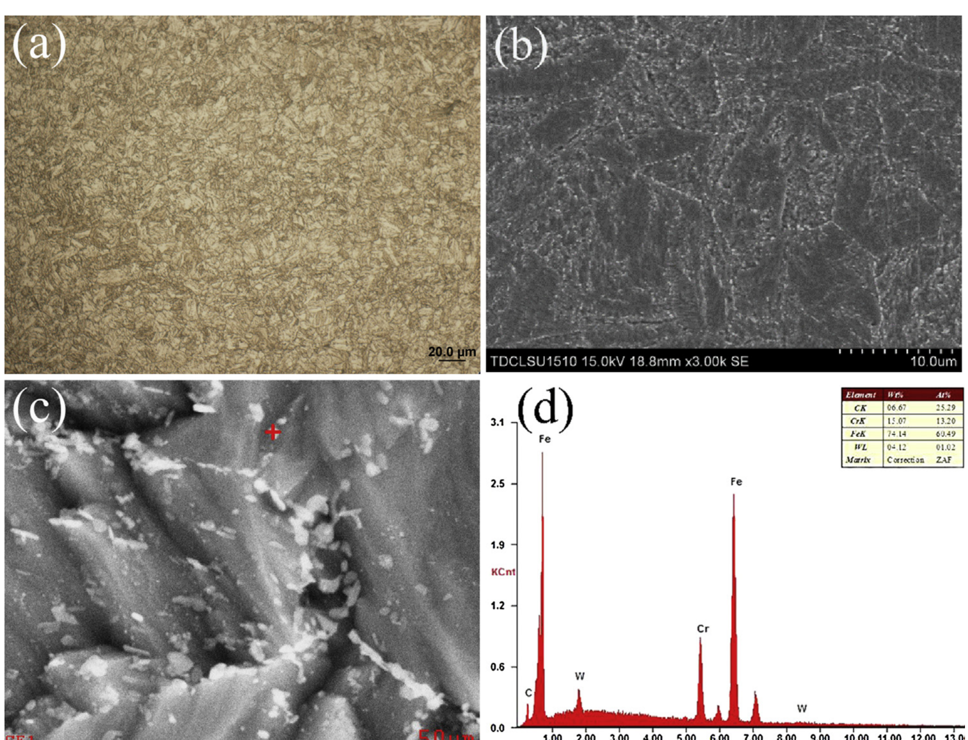

Fig 1. Microstructure of BM under (a) OM, (b) SEM, (c) $M_{23}C_6$ precipitation and (d) EDS map of the $M_{23}C_6$ precipitation.

Please cite this article in press as: C. Zhang, et al., J. Mater. Sci. Technol. (2017), https://doi.org/10.1016/j.jmst.2017.11.049